Frequency-domain evaluation of the adjoint Floquet eigenvectors for oscillator noise characterisation

# Frequency-domain evaluation of the adjoint Floquet eigenvectors for oscillator noise characterisation

*F.L. Traversa*[1] *F. Bonani*[2]

[1]*Departament d'Enginyeria Electrònica, Universitat Autònoma de Barcelona, 08193 Bellaterra (Barcelona), Spain*
[2]*Dipartimento di Elettronica, Politecnico di Torino, Corso Duca degli Abruzzi 24, 10129 Torino, Italy*
*E-mail: fabrizio.bonani@polito.it*

**Abstract:** The calculation of orbital fluctuations and of the phase-orbital correlation within Floquet-based noise analysis of autonomous systems requires the availability of all the direct and adjoint Floquet eigenvectors associated with the noiseless limit cycle. Here the authors introduce a novel numerical technique for their frequency domain determination. The algorithm is entirely based on the Jacobian matrices already available from the harmonic balance-based calculation of the limit cycle, thus avoiding any time-domain integration. The Floquet eigenvalues and adjoint eigenvectors are calculated from a generalised eigenvalue problem, thus making the approach readily implementable into CAD tools provided that the Jacobian matrices are made available.

## 1 Introduction

Noise analysis of oscillators has been the object of research for decades because of their widespread use in communication systems, and of the impact of oscillator noise on receiver sensitivity [1]. Recently, a mathematically rigorous noise analysis technique has been proposed in [2, 3], further developing the seminal approach in [4, 5]. The approach in [2] considers only phase noise in the output fluctuations, neglecting orbital noise which may in some cases become important [6]. The inclusion of orbital noise, and of the phase-orbit correlation, is treated in detail in [7], where we derive a full perturbative characterisation of oscillator phase and orbital noise in the case of white Gaussian noise sources (see also [8]). Other authors proposed different analyses in [4–6]: all these methods, however, share the same foundation, that is, Floquet theory applied to the linearised oscillator equations. In particular, in all cases the direct and adjoint (see the discussion later on) Floquet eigenvectors associated with the Floquet exponents of the unperturbed oscillator orbit are a basic ingredient for determining the noise spectrum (see also [9]).

In this contribution, we propose a novel frequency domain numerical algorithm, fully based on the harmonic balance (HB) technique and on the jacobian matrices exploited for its numerical implementation, which allows for an efficient estimation of the relevant quantities required for the calculation of the oscillator complete noise spectrum.

## 2 Glimpse on Floquet-based oscillator noise analysis

The theory developed in [2, 7] allows one to express the noise spectrum of an oscillator by exploiting a non-linear perturbation analysis around the noiseless oscillator limit cycle. Such a spectrum is decomposed into the phase noise contribution, the orbital (amplitude) fluctuations and their correlation. All these components are in turn given by a superposition of Lorentzian spectra around the harmonics of the fundamental frequency $f_0$. The parameters of the Lorentzian components (i.e. amplitude and corner frequency) depend, besides of course from the input noise sources, from the Floquet eigenvalues and eigenvectors of the direct and adjoint linear periodically time-varying (LPTV) system obtained linearising the oscillator dynamical equations around the noiseless orbit. Notice that, although with different final expressions for the spectra, this holds also for the other Floquet-based orbital noise theories proposed in [4–6], thus confirming the necessity to estimate all the Floquet quantities associated with the limit cycle.

The available orbital noise analyses are currently limited to the case of oscillators described by ordinary differential equations [4–7], although this is not the most general case because the modified nodal analysis of circuits, in general, leads to describing the system under consideration by means of differential-algebraic equations (DAEs) [10]. The Floquet-based analysis of phase noise has been formulated for DAEs in [11], whereas the extension of the methodology for orbital fluctuations analysis described in [7] is currently under development. Therefore here we consider the more general case of an autonomous circuit represented by an index-1 DAE [11]

$$\frac{\mathrm{d}}{\mathrm{d}t}\boldsymbol{q}(\boldsymbol{x}) - \boldsymbol{f}(\boldsymbol{x}) = \boldsymbol{0} \tag{1}$$

where $\boldsymbol{x}(t) \in \mathbb{R}^n$ is the state vector, and $\boldsymbol{q}(\cdot), \boldsymbol{f}(\cdot): \mathbb{R}^n \to \mathbb{R}^n$ are non-linear functions.

Assuming that (1) admits of a non-trivial periodic solution (limit cycle) $\boldsymbol{x}_S(t)$ of period $T$, the LPTV direct system derived by linearising (1) around $\boldsymbol{x}_S(t)$ is defined by

$$\frac{\mathrm{d}t}{\mathrm{d}t}[\boldsymbol{C}(t)\boldsymbol{z}(t)] - \boldsymbol{A}(t)\boldsymbol{z}(t) = \boldsymbol{0} \tag{2}$$

where the $T$-periodic $\boldsymbol{C}$ and $\boldsymbol{A}$ $n \times n$ matrices are the Jacobians of the non-linear functions $\boldsymbol{q}(\cdot)$ and $\boldsymbol{f}(\cdot)$ evaluated in the limit cycle. According to [11], we assume here that $\boldsymbol{C}(t)$ has a rank $m \leq n$ independent of time. The adjoint of (2) is [11]

$$\boldsymbol{C}^{\mathrm{T}}(t)\frac{\mathrm{d}t}{\mathrm{d}t}\boldsymbol{w}(t) + \boldsymbol{A}^{\mathrm{T}}(t)\boldsymbol{w}(t) = \boldsymbol{0} \tag{3}$$

The generalised Floquet theorem (Floquet theorem was originally derived for ordinary differential equations, and recently extended [11] to the case of index-1 DAEs.) valid for index-1 DAEs allows us to express the solution of (2) and (3), respectively, as

$$\boldsymbol{z}(t) = \mathrm{e}^{\mu_k t}\boldsymbol{u}_k(t) \quad \boldsymbol{w}(t) = \mathrm{e}^{-\mu_k t}\boldsymbol{v}_k(t) \quad k = 1, \ldots, n \tag{4}$$

where $\mu_k$ are the Floquet eigenvalues or exponents (FE) of the limit cycle, and $\boldsymbol{u}_k(t)$, $\boldsymbol{v}_k(t)$ are the $T$-periodic direct and adjoint Floquet eigenvectors. As for an autonomous system one of the FE is always equal to zero, we assume $\mu_1 = 0$; furthermore, the discussion in [11] shows that there are $n - m$ Floquet exponents $\mu_k = -\infty$, that we number as $k = m + 1, \ldots, n$. The two sets of vector functions $\boldsymbol{u}$ and $\boldsymbol{v}$ satisfy the generalised biorthogonality conditions

$$\boldsymbol{V}^{\mathrm{T}}(t)\boldsymbol{C}(t)\boldsymbol{U}(t) = \begin{bmatrix} \boldsymbol{I}_m & \boldsymbol{0} \\ \boldsymbol{0} & \boldsymbol{0} \end{bmatrix} \tag{5}$$

where

$$\boldsymbol{V}(t) = \left[\, \boldsymbol{v}_1(t), \ \ldots, \boldsymbol{v}_m(t), \boldsymbol{v}_{m+1}(t), \ \ldots, \boldsymbol{v}_n(t) \,\right] \tag{6}$$

$$\boldsymbol{U}(t) = \left[\, \boldsymbol{u}_1(t), \ \ldots, \boldsymbol{u}_m(t), \boldsymbol{u}_{m+1}(t), \ \ldots, \boldsymbol{u}_n(t) \,\right] \tag{7}$$

and $\boldsymbol{I}_m$ is the $m$-dimensional identity matrix.

According to the theory in [2, 7], phase noise is fully characterised by the perturbation projection vector (PPV) $\boldsymbol{v}_1(t)$ through the constant

$$c = \frac{1}{T}\int_0^T \boldsymbol{v}_1^{\mathrm{T}}(t)\boldsymbol{B}(\boldsymbol{x}_S)\boldsymbol{B}^{\mathrm{T}}(\boldsymbol{x}_S)\boldsymbol{v}_1(t)\,\mathrm{d}t \tag{8}$$

while the orbital and phase-orbit correlation components of the spectrum depend on the other eigenvalues $\mu_k$ and (direct and adjoint, respectively) eigenvectors $\boldsymbol{u}_k(t)$ and $\boldsymbol{v}_k(t)$. We shall extend the term PPV to all the adjoint eigenvectors $\boldsymbol{v}_k(t)$, because they provide the projection versors along the Floquet decomposition of the oscillator orbit.

Once the limit cycle is known, the most common approach to the numerical evaluation of the FEs and of the $\boldsymbol{u}$ and $\boldsymbol{v}$ sets is based on the time-domain determination of the monodromy matrix for the direct and adjoint systems, respectively, (see [12, Chapter 10] and [6, 11, 13]), which is difficult and quite time consuming. The main problem is related to the exponential dependence in (4) which is growing with time since, for a stable oscillator, $\mathrm{Re}\{\mu_k\} \leq 0$ for $k > 1$. This amplifies the accumulated discretisation error unless special integration techniques are exploited (see also the discussion in [12, Chapter 10]). On the other hand, in [14] numerical techniques are presented for the efficient time- and frequency-domain determination of the $k = 1$ PPV only, based on the exploitation of an augmented version of the Jacobian matrices involved in the LPTV system definition. Notice that such matrices are also very often used for the determination of the limit cycle $\boldsymbol{x}_S(t)$.

## 3 Frequency-domain algorithm

Here we present a novel numerical technique for frequency-domain determination of the entire $\boldsymbol{v}$ set, based on the HB method. This approach, founded on the methodology presented in [15, 16], allows us to estimate the frequency representation of the $\boldsymbol{v}_k$ vectors as the result of an eigenvalue problem, exploiting the same matrices already used in the Newton's solution of the HB system leading to the limit cycle calculation. Notice that the $\boldsymbol{u}$ set can be determined, in a quite similar way, by means of the algorithm discussed in [15].

In order to introduce the frequency-domain determination of the $\boldsymbol{v}$ vector set, let us substitute into (3) the general form of the solution $\boldsymbol{w}(t) = \exp(-\mu_k t)\boldsymbol{v}_k(t)$, obtaining

$$-\mu_k \boldsymbol{C}^{\mathrm{T}}(t)\boldsymbol{v}_k(t) + \boldsymbol{C}^{\mathrm{T}}(t)\dot{\boldsymbol{v}}_k(t) + \boldsymbol{A}^{\mathrm{T}}(t)\boldsymbol{v}_k(t) = \boldsymbol{0} \tag{9}$$

where $\dot{\boldsymbol{v}}$ denotes the time derivative.

The HB technique requires sampling the $T$-periodic functions in $(2N + 1)$ time samples $t_j$ distributed within an interval of width $T$. Each vector function $\boldsymbol{x}(t) \in \mathbb{R}^n$ is therefore transformed into a $n(2N + 1)$ vector $\hat{\boldsymbol{x}}$ built collecting the time samples $\hat{\boldsymbol{x}}_i = [x_i(t_1) \ldots x_i(t_{2N+1})]^{\mathrm{T}}$ for each component $x_i(t)$

$$\hat{\boldsymbol{x}}^{\mathrm{T}} = [\hat{\boldsymbol{x}}_1^{\mathrm{T}}, \ \ldots, \hat{\boldsymbol{x}}_n^{\mathrm{T}}] \tag{10}$$

A similar procedure is carried out on matrices: let $X_{i,j}(t)$ be the $(i, j)$th element of matrix $\boldsymbol{X}(t) \in \mathbb{R}^{n \times n}$. The sampled version of the element is a diagonal matrix built with the time samples of $X_{i,j}(t)$: $\hat{\boldsymbol{X}}_{i,j} = \mathrm{diag}\{X_{i,j}(t_1) \ldots X_{i,j}(t_{2N+1})\}$, whereas time sampling of the entire matrix leads to the $n(2N + 1) \times n(2N + 1)$ matrix built of diagonal blocks

$$\hat{\boldsymbol{X}} = \begin{bmatrix} \hat{\boldsymbol{X}}_{1,1} & \ldots & \hat{\boldsymbol{X}}_{1,n} \\ \vdots & \ddots & \vdots \\ \hat{\boldsymbol{X}}_{n,1} & \ldots & \hat{\boldsymbol{X}}_{n,n} \end{bmatrix} \tag{11}$$

According to [10], the HB formulation amounts to represent each time-sampled function with the corresponding harmonic (Fourier) amplitudes

$$x_i(t) = x_{i,c0} + \sum_{h=1}^{N} [x_{i,\mathrm{ch}} \cos(h\omega_0 t) + x_{i,\mathrm{sh}} \sin(h\omega_0 t)] \tag{12}$$

where $\omega_0 = 2\pi f_0$. The relationship between the time samples

and the harmonic amplitudes is given by the DFT operator

$$\boldsymbol{\Gamma}^{-1} = \begin{bmatrix} 1 & \gamma^{\mathrm{c}}_{1,1} & \gamma^{\mathrm{s}}_{1,1} & \cdots & \gamma^{\mathrm{c}}_{1,N} & \gamma^{\mathrm{s}}_{1,N} \\ \vdots & \vdots & \vdots & \ddots & \vdots & \vdots \\ 1 & \gamma^{\mathrm{c}}_{2N+1,1} & \gamma^{\mathrm{s}}_{2N+1,1} & \cdots & \gamma^{\mathrm{c}}_{2N+1,N} & \gamma^{\mathrm{s}}_{2N+1,N} \end{bmatrix} \tag{13}$$

where

$$\gamma^{\mathrm{c}}_{p,q} = \cos(q\omega_0 t_p) \quad \gamma^{\mathrm{s}}_{p,q} = \sin(q\omega_0 t_p) \tag{14}$$

Collecting the harmonic amplitudes into $\tilde{\boldsymbol{x}}_i = [x_{i,\mathrm{c}0}, x_{i,\mathrm{c}1}, x_{i,\mathrm{s}1}, \ldots, x_{i,\mathrm{c}N}, x_{i,\mathrm{s}N}]^{\mathrm{T}}$, one finds

$$\hat{\boldsymbol{x}}_i = \boldsymbol{\Gamma}^{-1}\tilde{\boldsymbol{x}}_i \Longleftrightarrow \tilde{\boldsymbol{x}}_i = \boldsymbol{\Gamma}\hat{\boldsymbol{x}}_i \tag{15}$$

To generalise (15) to vector functions, we define the block-diagonal linear operator $\boldsymbol{\Gamma}_n = \mathrm{diag}\{\boldsymbol{\Gamma}, \ldots, \boldsymbol{\Gamma}\}$ built of $n$ copies of $\boldsymbol{\Gamma}$, so that

$$\hat{\boldsymbol{x}} = \boldsymbol{\Gamma}_n^{-1}\tilde{\boldsymbol{x}} \Longleftrightarrow \tilde{\boldsymbol{x}} = \boldsymbol{\Gamma}_n\hat{\boldsymbol{x}} \tag{16}$$

The last operator needed is the representation in the HB basis of time derivation. The harmonic amplitudes of the scalar function $\dot{x}_i(t)$ are easily derived as [15]

$$\tilde{\dot{\boldsymbol{x}}}_i = \boldsymbol{\Gamma}\hat{\dot{\boldsymbol{x}}}_i = \omega_0\boldsymbol{\Omega}\tilde{\boldsymbol{x}}_i \tag{17}$$

where

$$\boldsymbol{\Omega} = \begin{bmatrix} 0 & 0 & 0 & 0 & 0 & \ldots & 0 & 0 \\ 0 & 0 & 1 & 0 & 0 & \ldots & 0 & 0 \\ 0 & -1 & 0 & 0 & 0 & \ldots & 0 & 0 \\ 0 & 0 & 0 & 0 & 2 & \ldots & 0 & 0 \\ 0 & 0 & 0 & -2 & 0 & \ldots & 0 & 0 \\ \vdots & \vdots & \vdots & \vdots & \vdots & \ddots & \vdots & \vdots \\ 0 & 0 & 0 & 0 & 0 & \ldots & 0 & N \\ 0 & 0 & 0 & 0 & 0 & \ldots & -N & 0 \end{bmatrix} \tag{18}$$

Again, the extension to the case of a vector function requires to define the block-diagonal derivation operator $\boldsymbol{\Omega}_n = \mathrm{diag}\{\boldsymbol{\Omega}, \ldots, \boldsymbol{\Omega}\}$ built of $n$ copies of $\boldsymbol{\Omega}$

$$\tilde{\dot{\boldsymbol{x}}} = \omega_0\boldsymbol{\Omega}_n\tilde{\boldsymbol{x}} \tag{19}$$

Time-discretisation of (9) leads to

$$-\mu_k\hat{\boldsymbol{C}}^{\mathrm{T}}\hat{\boldsymbol{v}}_k + \hat{\boldsymbol{C}}^{\mathrm{T}}\hat{\dot{\boldsymbol{v}}}_k + \hat{\boldsymbol{A}}^{\mathrm{T}}\hat{\boldsymbol{v}}_k = \boldsymbol{0} \tag{20}$$

where, according to (11)

$$\hat{\boldsymbol{X}}^{\mathrm{T}} = \begin{bmatrix} \hat{\boldsymbol{X}}^{\mathrm{T}}_{1,1} & \cdots & \hat{\boldsymbol{X}}^{\mathrm{T}}_{n,1} \\ \vdots & \ddots & \vdots \\ \hat{\boldsymbol{X}}^{\mathrm{T}}_{1,n} & \cdots & \hat{\boldsymbol{X}}^{\mathrm{T}}_{n,n} \end{bmatrix} = \begin{bmatrix} \hat{\boldsymbol{X}}_{1,1} & \cdots & \hat{\boldsymbol{X}}_{n,1} \\ \vdots & \ddots & \vdots \\ \hat{\boldsymbol{X}}_{1,n} & \cdots & \hat{\boldsymbol{X}}_{n,n} \end{bmatrix} \tag{21}$$

since the building blocks are diagonal. Multiplying (20) from the left by $\boldsymbol{\Gamma}_n$ and using (16), (19) leads to the frequency-domain representation of the equation defining the FE and the eigenvectors $\boldsymbol{v}_k(t)$

$$-\mu_k\tilde{\boldsymbol{C}}_{\mathrm{T}}\tilde{\boldsymbol{v}}_k + \omega_0\tilde{\boldsymbol{C}}_{\mathrm{T}}\boldsymbol{\Omega}_n\tilde{\boldsymbol{v}}_k + \tilde{\boldsymbol{A}}_{\mathrm{T}}\tilde{\boldsymbol{v}}_k = \boldsymbol{0} \tag{22}$$

where

$$\tilde{\boldsymbol{C}}_{\mathrm{T}} = \boldsymbol{\Gamma}_n\hat{\boldsymbol{C}}^{\mathrm{T}}\boldsymbol{\Gamma}_n^{-1} \quad \tilde{\boldsymbol{A}}_{\mathrm{T}} = \boldsymbol{\Gamma}_n\hat{\boldsymbol{A}}^{\mathrm{T}}\boldsymbol{\Gamma}_n^{-1} \tag{23}$$

Therefore the $\boldsymbol{v}_k$ set is made of the eigenvectors of the generalised eigenvalue problem

$$[\omega_0\tilde{\boldsymbol{C}}_{\mathrm{T}}\boldsymbol{\Omega}_n + \tilde{\boldsymbol{A}}_{\mathrm{T}}]\tilde{\boldsymbol{v}}_k = \mu_k\tilde{\boldsymbol{C}}_{\mathrm{T}}\tilde{\boldsymbol{v}}_k \tag{24}$$

Notice that matrices $\tilde{\boldsymbol{C}}_{\mathrm{T}}$ and $\tilde{\boldsymbol{A}}_{\mathrm{T}}$ defined in (23) are simply a permutation of matrices $\tilde{\boldsymbol{C}} = \boldsymbol{\Gamma}_n\hat{\boldsymbol{C}}\boldsymbol{\Gamma}_n^{-1}$ and $\tilde{\boldsymbol{A}} = \boldsymbol{\Gamma}_n\hat{\boldsymbol{A}}\boldsymbol{\Gamma}_n^{-1}$ used for the direct eigenvectors calculation [15], respectively, since from (21)

$$\tilde{\boldsymbol{X}}_{\mathrm{T}} = \boldsymbol{\Gamma}_n\hat{\boldsymbol{X}}^{\mathrm{T}}\boldsymbol{\Gamma}_n^{-1} = \begin{bmatrix} \tilde{\boldsymbol{X}}_{1,1} & \cdots & \tilde{\boldsymbol{X}}_{n,1} \\ \vdots & \ddots & \vdots \\ \tilde{\boldsymbol{X}}_{1,n} & \cdots & \tilde{\boldsymbol{X}}_{n,n} \end{bmatrix} \tag{25}$$

Accordingly, (24) involves the same block components already exploited in the HB system solution leading to the determination of $\boldsymbol{x}_{\mathrm{S}}(t)$, at least if Newton's method is employed.

The full solution of the generalised eigenvalue problem (24) yields $n(2N+1)$ eigenvalues, distributed in the complex plane in 'vertical' lines characterised by the same (apart from numerical errors) real part: according to the discussion in [15], numerical precision considerations allow one to choose the values nearer to the real axis as the best representation of the actual $n$ FEs. This means that the relevant generalised eigenvalues are those located in a strip of the complex plane defined by the condition $-\omega_0/2 \le \mathrm{Im}\{\mu_k\} \le \omega_0/2$, and therefore specialised algorithms for their determination as those discussed in [17] can be exploited. With respect to the numerical method proposed in [14], (24) has two advantages: all the eigenvectors can be calculated, thus making possible the characterisation of the orbital deviation besides phase noise, and no augmented Jacobian should be built. On the other hand, the algorithm in [14] directly evaluates the PPV, thus avoiding the numerical issues corresponding to the correct choice of $\hat{\boldsymbol{v}}_1$ whenever there are several eigenvalues near to zero. Nevertheless, the burden required by this choice is not overly significant, because use can be made of the biorthogonality relations (5) (see also [11, 14]): $\mu_1$ is chosen by picking up the eigenvalue that better satisfies the condition

$$\boldsymbol{v}_1^{\mathrm{T}}(t)\boldsymbol{C}(t)\boldsymbol{u}_1(t) = \boldsymbol{v}_1^{\mathrm{T}}(t)\boldsymbol{C}(t)\dot{\boldsymbol{x}}_{\mathrm{S}}(t) = 1 \tag{26}$$

as $\boldsymbol{u}_1(t) = \dot{\boldsymbol{x}}_{\mathrm{S}}(t)$ [2].

An HB-based procedure for the estimation of the FEs and of the direct Floquet eigenvectors was also proposed in [18], where the numerical procedure involves some matrix manipulations that might, in critical cases, reduce the numerical accuracy of the FEs (see Section 4.1). On the other hand, we make use of the Jacobian matrix in direct and permuted form.

## 4 Examples

We consider here two examples of application of the algorithm described in Section 3. In both cases, we make use of the estimation of the relative error of the limit cycle, Floquet eigenvectors and Floquet exponents defining the relative errors as follows ($1 \leq k \leq n$ denotes the number of FEs included in the estimation of the relative error, $j_i$ denotes the $i$th FE included in the error calculation)

$$\epsilon_{x_S} = \frac{\|x_S(N) - \bar{x}_S\|}{\|\bar{x}_S\|} \tag{27}$$

$$\epsilon_{v,k} = \max_{i=1,\ldots,k} \frac{\|v_{j_i}(N) - \bar{v}_{j_i}\|}{\|\bar{v}_{j_i}\|} \tag{28}$$

$$\epsilon_{\mu,k} = \frac{\max_{i=1,\ldots,k} |\mu_{j_i}(N) - \bar{\mu}_{j_i}|}{\max_{i=1,\ldots,k} |\bar{\mu}_{j_i}|} \tag{29}$$

where $\bar{x}$ denotes the 'exact' value of $x$, estimated as the solution of the HB method for large $N$, and $\|\cdot\|$ is the $L_2$ norm in $\mathbb{R}^n$. The choice in (29) is because of the fact that the maximu accuracy for an eigenvalue is related to the radius $\rho$ of the spectrum of the matrix, that is, to the largest (in magnitude) eigenvalue, and to the number $d$ of digits used for its representation (see [13, 19]), by

$$\epsilon = \rho \times 10^{-d} \tag{30}$$

Notice that $\epsilon_{\mu,1}$ reduces to the absolute value of $\mu_1$ when we consider the error associated to the nominally zero FE only.

### 4.1 Tow–Thomas oscillator

The first example is the Tow–Thomas oscillator presented in [18] and shown in Fig. 1. This example was chosen to allow for a comparison of the present approach with [18], where an algorithm for the frequency-domain evaluation of the Floquet eigenvalues and direct eigenvectors was also presented. The operational amplifiers are ideal and represented by nullors, while the inverter is approximated by the input–output relation $v_{out} = \tanh(-\alpha v_{in})$, where $\alpha$ is a parameter representing the slope of the transition. The circuit has $n = 3$ and $m = 2$, and therefore one of the FE is $-\infty$. To allow for a comparison with [18], we consider an HB simulation with 32 harmonics plus DC, and we set $\alpha = -3$. The resulting oscillation frequency is

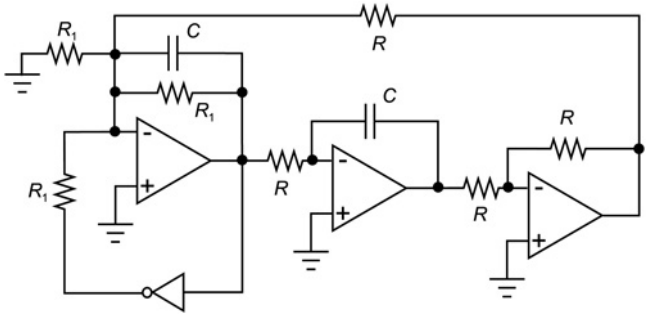


**Fig. 1** *Circuit of Tow–Thomas oscillator discussed in [18]*

Operational amplifiers are ideal and realised as nullors, while $R_1 = 3\,\text{k}\Omega$, $C = 20\,\text{nF}$. The input–output relation of the inverter is approximated through a tanh function

$f_0 = 7.91723\,\text{kHz}$, with the two Floquet exponents

$$\mu_1 = 8.9389851968458 \times 10^{-11} \simeq 0 \tag{31}$$

$$\mu_2 = -7737.1409649406 \tag{32}$$

Notice that, with the same number of harmonics, $\mu_2$ is in excellent agreement with [18], whereas our estimate of $\mu_1$ is five orders of magnitude lower.

This accuracy improvement is confirmed by an analysis of the error associated to the calculation of the limit cycle and of the corresponding Floquet eigenvalues and adjoint eigenvectors ($\epsilon_{\mu,1}$ and $\epsilon_{v,1}$), shown in Figs. 2 and 3 as a function of the number of harmonics used in the simulation. The 'exact' value was here estimated as the solution of the HB method for $N = 101$. The results clearly show that with our method the minimum error in the determination of the Floquet eigenvalues is obtained for a comparatively low number of harmonics, that is, $N \simeq 30$.

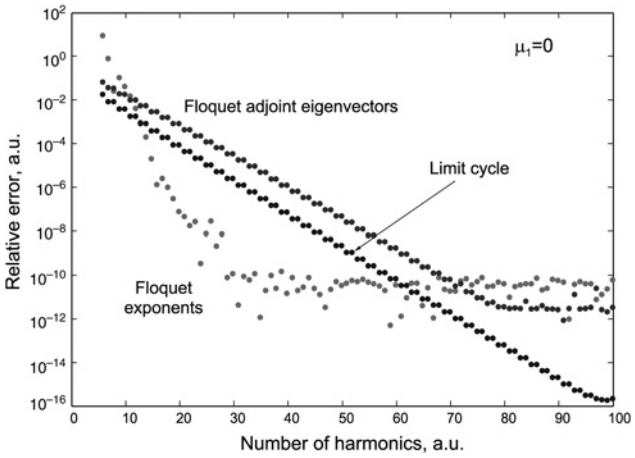


**Fig. 2** *Relative error for the determination of the limit cycle and of the Floquet adjoint eigenvector, and absolute error for the Floquet eigenvalue $\mu_1$ of the Tow–Thomas oscillator as a function of the number of harmonics in the HB simulation*

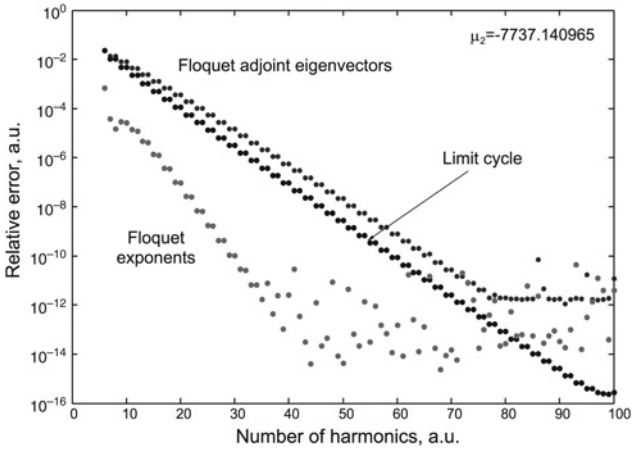


**Fig. 3** *Relative error for the determination of the limit cycle, of the Floquet adjoint eigenvector, and of the Floquet eigenvalue $\mu_2$ of the Tow–Thomas oscillator as a function of the number of harmonics in the HB simulation*

### 4.2 Colpitts oscillator

The second example is the Colpitts oscillator in Fig. 4. The bipolar transistor is described by the simplified model

$$i_B = I_S[e^{v_B/V_T} - 1] \quad i_C = \beta_F i_B \tag{33}$$

where $I_S = 8.8 \times 10^{-14}$ A, $V_T = 26$ mV and $\beta_F = 100$. The circuit parameters are: $V_{CC} = 15$ V, $R_1 = 28.6$ kΩ, $R_2 = 1.4$ kΩ, $R_C = 50$ Ω, $C_1 = 20$ nF, $C_2 = 1$ nF, $C_S = 1$ μF and $L = 83.556$ μH. The circuit has $m = n = 4$, and has been simulated with the HB technique. Using 120 harmonics plus DC, the oscillation frequency is $f_0 = 424.405$ kHz and the solution is shown in Fig. 5.

Exploiting the algorith in Section 3, we calculated the four Floquet eigenvalues of the limit cycle

$$\mu_1 = -2.11347673135426 \times 10^{-3} \simeq 0 \tag{34}$$

$$\mu_2 = -1.37828290506221 \tag{35}$$

$$\mu_3 = -1.62162555328646 \times 10^{5} \tag{36}$$

$$\mu_4 = -2.09408355672130 \times 10^{7} \tag{37}$$

and the correspondig Floquet eigenvector sets $\boldsymbol{u}$ and $\boldsymbol{v}$. As all the eigenvalues (apart from $\mu_1$ which is chosen, besides being the smallest in magnitude, because the associated eigenvectors better satisfy the biorthogonality condition (26)) exhibit negative real part, the limit cycle is stable. A 3D section in the state space of the normalised adjoint eigenvectors is shown in Fig. 6, using (5) as normalisation conditions.

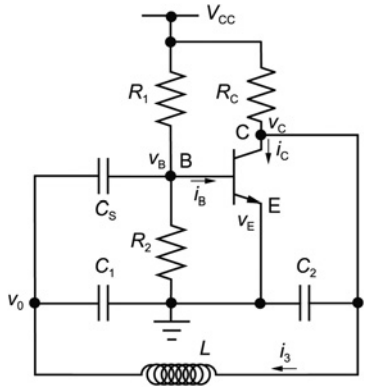


**Fig. 4** *Circuit of the Colpitts oscillator*

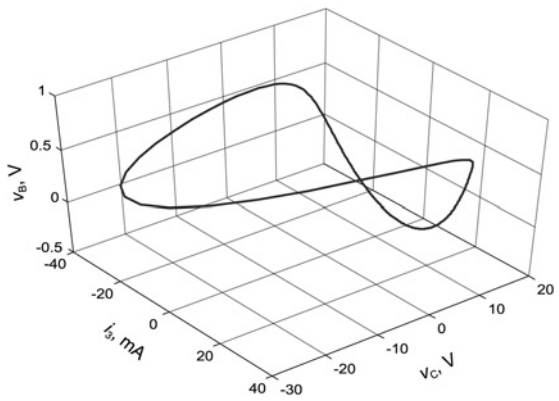


**Fig. 5** *3D section of the state-space limit cycle for the Colpitts oscillator*

We show in Fig. 7 a representation of the $N$ dependence of the relative error of the limit cycle ($\epsilon_{x_S}$), Floquet eigenvectors ($\epsilon_{v,4}$) and Floquet exponents ($\epsilon_{\mu,4}$) estimation where the 'exact' values are calculated as the solution of the HB method for $N = 161$.

The error analysis of both examples clearly shows that the truncation error is an exponentially decreasing function of $N$, thus suggesting that the HB technique is well suited for the accurate calculation of all of the Floquet quantities. This should be compared to the fact that, at least for the limit cycle determination, time-domain algorithms, such as the shooting technique, exhibit a truncation error which decreases polynomially with the number of time samples used to represent the cycle [12].

Using the Floquet eigenvalues and eigenvectors discussed above, we calculated the full noise spectrum of the circuit assuming as a noise source the shot noise generators of the bipolar transistor and exploiting the technique presented in [7, 8]. The result is shown in Fig. 8 as a function of the absolute frequency. The phase noise contribution is dominant near to the limit cycle harmonics, whereas the orbital contribution is important far from $qf_0$ ($q$ integer). Notice that the orbital noise is responsible of the non-symmetric spectrum shape between the cycle harmonics (as

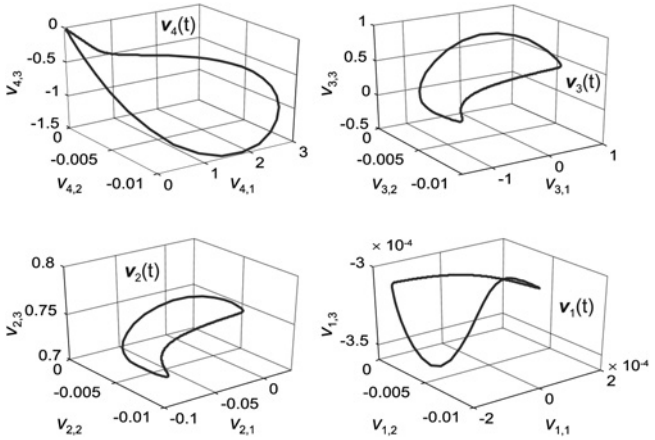


**Fig. 6** *3D section of the state-space adjoint eigenvectors* $\boldsymbol{v}$ *for the Colpitts oscillator*

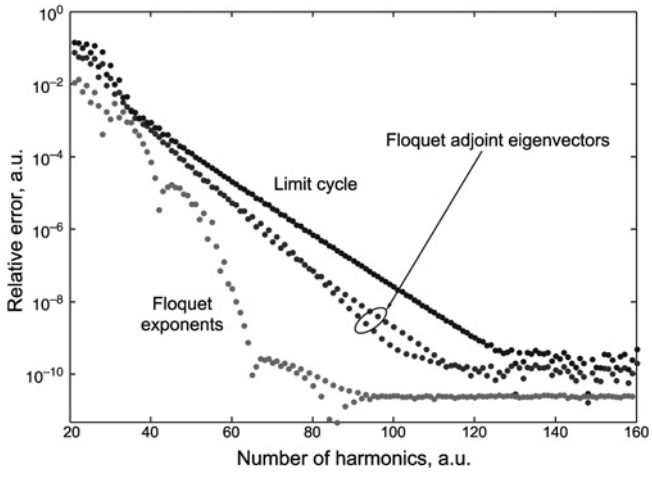


**Fig. 7** *Relative error in the limit cycle, Floquet adjoint eigenvectors and Floquet eigenvalues determination as a function of the number of harmonics included in the HB simulation for the Colpitts oscillator*

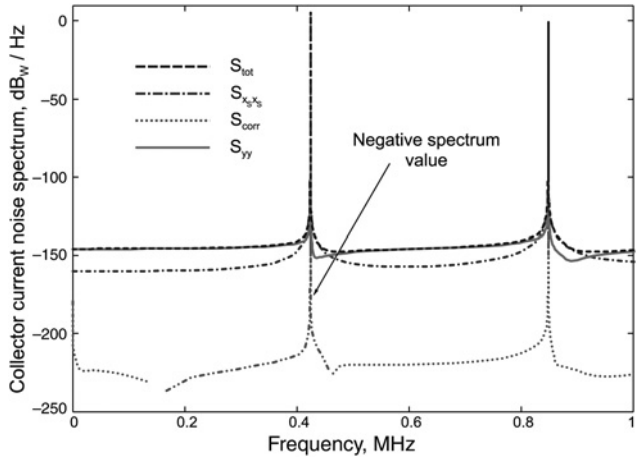


**Fig. 8** *Collector current noise spectrum of the Colpitts oscillator as a function of the absolute frequency for the Colpitts oscillator*

found also in [20]), and its frequency dependence is not Lorentzian around the harmonics because of the superposition of several Lorentzian terms. Furthermore, the correlation between phase and orbital fluctuations is, at least for this example, negligible.

The asymmetry provided by the orbital noise is even more evident observing the upper and lower sidebands around the fundamental, shown in Fig. 9. Also the correlation

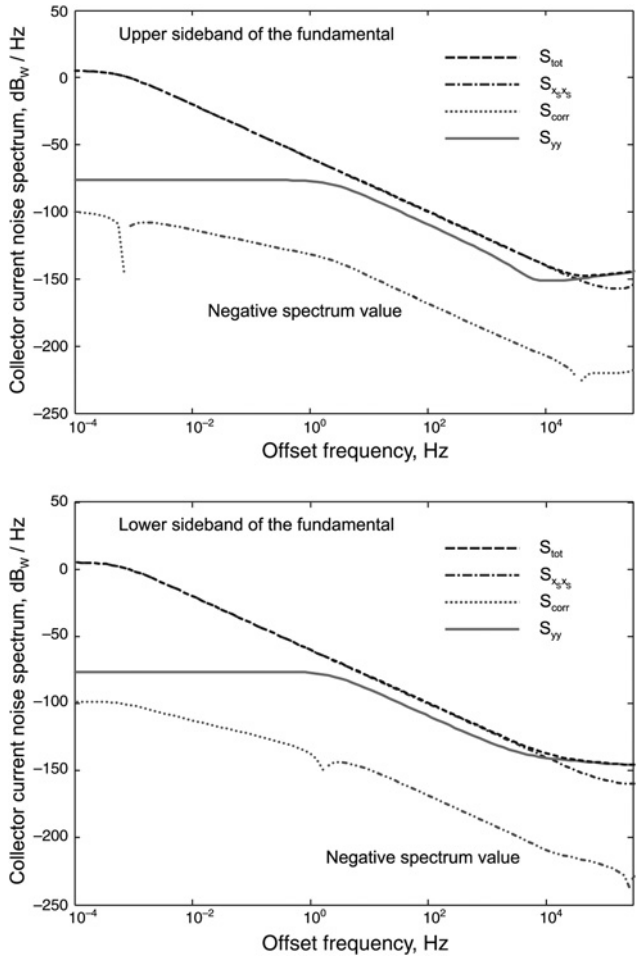


**Fig. 9** *Upper (above) and lower (below) sideband frequency dependence of the collector current noise spectrum of the Colpitts oscillator around the fundamental frequency $f_0$*

contribution is neither Lorentzian in shape, nor symmetric with respect to $f_0$.

## 5 Conclusions

We presented a novel algorithm for the numerical calculation of the Floquet adjoint eigenvectors based on the HB technique, and therefore readily implementable in most CAD tools for RF/microwave analysis and design. The numerical technique exploits the Jacobian matrices already used in the Newton cycle typically used to solve the HB problem, and makes available the quantities necessary for the estimation of the oscillator orbital fluctuations and of their correlation with phase noise.

## 6 References


1 Hajimiri, A., Lee, T.H.: 'The design of low noise oscillators' (Kluwer Academic Publishers, 1999)

2 Demir, A., Mehrotra, A., Roychowdhury, J.: 'Phase noise in oscillators: a unifying theory and numerical methods for characterization', *IEEE Trans. Circuits Syst. I, Fundam. Theory Appl.*, 2000, **47**, (5), pp. 655–674

3 Demir, A.: 'Phase noise and timing jitter in oscillators with colored-noise sources', *IEEE Trans. Circuits Syst. I, Fundam. Theory Appl.*, 2000, **49**, (12), pp. 1782–1791

4 Kärtner, F.K.: 'Determination of the correlation spectrum of oscillators with low noise', *IEEE Trans. Microw. Theory Tech.*, 1989, **37**, (1), pp. 90–101

5 Kärtner, F.K.: 'Analysis of white and $f^{-\alpha}$ noise in oscillators', *Int. J. Circuit Theory Appl.*, 1990, **18**, pp. 485–519

6 Carbone, A., Palma, F.: 'Considering noise orbital deviations on the evaluation of power density spectrum of oscillators', *IEEE Trans. Circuits Syst. II, Express Briefs*, 2006, **53**, (6), pp. 438–442

7 Traversa, F.L., Bonani, F.: 'Oscillator noise: a nonlinear perturbative theory including orbital fluctuations and phase-orbital correlation', *IEEE Trans. Circuits Syst. I, Regul. Pap.*, submitted

8 Traversa, F.L., Bonani, F.: 'Oscillator noise: a rigorous analysis including orbital fluctuations'. Proc. Integrated Nonlinear Microwave and Millimetre-wave Circuits, Göteborg, Sweden, April 2010, pp. 126–129

9 Coram, G.J.: 'A simple 2-D oscillator to determine the correct decomposition of perturbations into amplitude and phase noise', *IEEE Trans. Circuits Syst. I*, 2001, **48**, pp. 896–898

10 Kundert, K.S., Sangiovanni-Vincentelli, A., White, J.K.: 'Steady-state methods for simulating analog and microwave circuits' (Kluwer Academic Publisher, 1990)

11 Demir, A.: 'Floquet theory and non-linear perturbation analysis for oscillators with differential-algebraic equations', *Int. J. Circuit Theory Appl.*, 2000, **28**, pp. 163–185

12 Kuznetsov, Y.A.: 'Elements of applied bifurcation theory' (Springer Verlag, 1998, 2nd edn.)

13 Lust, K.: 'Improved numerical Floquet multipliers', *Int. J. Bifurcation Chaos*, 2001, **11**, (9), pp. 2389–2410

14 Demir, A., Roychowdhury, J.: 'A reliable and efficient procedure for oscillator PPV computation, with phase noise macromodeling applications', *IEEE Trans. CAD*, 2003, **22**, (2), pp. 188–197

15 Traversa, F.L., Bonani, F., Donati Guerrieri, S.: 'A frequency-domain approach to the analysis of stability and bifurcations in nonlinear systems described by differential-algebraic equations', *Int. J. Circuit Theory Appl.*, 2008, **36**, (4), pp. 421–439

16 Traversa, F.L., Bonani, F.: 'A novel numerical approach for the frequency-domain calculation of oscillator noise'. Proc. 20th Int. Conf. on Noise and Fluctuations, Pisa, Italy, June 2009, pp. 497–500

17 Tisseur, F., Meerbergen, K.: 'The quadratic eigenvalue problem', *SIAM Rev.*, 2001, **43**, (2), pp. 235–286

18 Brambilla, A., Gruosso, G., Storti Gajani, G.: 'Determination of Floquet exponents for small-signal analysis of nonlinear periodic circuits', *IEEE Trans. Comput. Aided Des. Integr. Circuits Syst.*, 2009, **28**, (3), pp. 447–451

19 Golub, G.H., van Loan, C.F.: 'Matrix computations' (The Johns Hopkins University Press, 1996, 3rd edn.)

20 Brambilla, A., Gruosso, G., Redaelli, M.A., Storti Gajani, G., Caviglia, D.D.: 'Improved small signal analysis for circuits working in periodic steady state', *IEEE Trans. Circuits Syst. I, Regul. Pap.*, 2010, **57**, (2), pp. 427–437